Numerical study of fast ion behavior in the presence of magnetic islands and toroidal field ripple in the EAST tokamak*

Zhang Wei(张 伟), Hu Li-Qun(胡立群)†, Sun You-Wen(孙有文),
Ding Si-Ye(丁斯晔), Zhang Zi-Jun(张子君), and Liu Song-Lin(刘松林)

Institute of Plasma Physics, Chinese Academy of Sciences, Hefei 230031, *China*

(Received 5 March 2014; revised manuscript received 16 April 2014; published online 10 August 2014)

A peculiar first orbit loss type was found apart from the normal ones when we use ORBIT code to simulate fast ion orbits in the EAST tokamak. Fast ion orbits were studied in the presence of toroidal field (TF) ripple and magnetohydrodynamic (MHD) perturbations. We analyzed the properties of the drifted orbits in detail and compared their differences, finding that the combined effects of ripple and magnetic islands are much greater than the effects of either one of them alone. Then we investigated the orbit deviations as a function of pitch angle in different radial positions. The modeling results demonstrate that the loss of trapped particles is mainly caused by the ripple, while MHD perturbation mainly plays an important role in the passing particles. Furthermore we modeled the loss rate using different equilibriums. Results prove that a higher beta can indeed improve the confinement of fast ions, while a little change in the q profile can make the topologies of magnetic islands become quite different and results in quite different total particle losses.

Keywords: fast ion, toroidal field ripple, magnetic island, orbit drift

PACS: 52.20.Dq, 52.65.–y, 52.25.Fi **DOI:** 10.1088/1674-1056/23/10/105201

1. Introduction

Energetic particle is an important topic in fusion science and has gathered extensive interest in the past. For future tokamaks such as ITER, self-sustained ignition greatly depends on heating by highly energetic alpha particles produced from fusion reactions.[1] In present tokamaks energetic particles are mainly generated from neutral beam injection (NBI) and radio frequency (RF) heating. A good confinement of energetic particles is necessary for good plasma performance. The loss of these particles can be very harmful: the heating efficiency would be affected, the wall would be damaged, and impurities caused from the wall can be a great threat to the plasma. Thus the study of the behavior of fast ions is important; a full understanding of them enables us to find a better way to control them. The purpose of this article is to investigate the behaviors of fast ions under ripple and magnetic islands in the EAST tokamak machine, research the loss channels and loss rates under different conditions, and provide helpful suggestions for a better confinement.

Previously, lots of studies focused on particle behaviors in the presence of TF ripple[2–7] and magnetic modes.[8–12] Unlike those studies, we implemented new ways in our studies. We, not only comprehensively studied the drift orbits of trapped and passing particles, but also quantitatively studied orbit deviations and related loss domains, and further researched the important factors that affect the total loss. Many comparisons between the magnetic islands' effects and ripple effects are made in the paper, together with their relevant loss channels.

The experimental Advanced Superconducting Tokamak (EAST) is a fully superconducting magnetic confinement device used for nuclear fusion studies in China. ORBIT code, which is based on the theory of guiding center motion[13,14] is used in the paper for most of the modeling work. In ORBIT code we regard particles that hit the last closed flux surface (LCFS) as lost. But because orbits that go through the gap between last closed flux surface and wall may reenter the plasma domain, the number of lost particles counted would be a little overestimated. Since we mainly studied the fast ion behavior in the core plasmas, and focused on the comparison of the lost particles in cases of different experimental parameters, this influence is beyond our consideration.

The paper is organized as follows. In Section 2 the orbit drifts caused by the toroidal field ripple and magnetohydrodynamic perturbation are explicitly studied and compared. In Section 3 orbit deviations as a function of pitch angle and radial position are calculated, and the domains of lost particles in the μ–P_ς plane are given. Total losses under different equilibriums are simulated in Section 4, while the importance of several experimental parameters is also analyzed. The main results are summarized in the final section.

*Project supported by the JSPS-NRF-NSFC A3 Foresight Program in the Field of Plasma Physics (NSFC Grant No. 11261140328).
†Corresponding author. E-mail: lqhu@ipp.ac.cn
© 2014 Chinese Physical Society and IOP Publishing Ltd

2. Orbit drifts induced by magnetic islands and ripple

An 80-keV deuterium ion was chosen as the test ion for our studies, which is a very ordinary case during the additional heatings in EAST tokamak. The equilibriums used in the modeling work are all obtained from shot 36662 and 36770. The experimental parameters of these two shots are listed in Table 1. We use equilibriums (shot 36662) for the modeling works in Sections 2 and 3, and equilibriums (shot 36770) in Section 4. Shown in Fig. 1(a) is the equilibrium (shot 36662) plotted in Boozer coordinate. Figure 1(b) shows the safety factor q profile of this equilibrium, and the MHD perturbation profile used later.

Table 1. Experimental parameters of the two shots.

Shot	Major radius R/m	Minor radius a/m	Toroidal field B_t/T	Plasma density N_{e0}/m^{-3}	Plasma temperature T_{e0}/keV	Plasma current I_p/kA
36662	1.874	0.445	2.012	2.6×10^{19}	0.74	400
36770	1.873	0.443	2.011	3.2×10^{19}	1	400

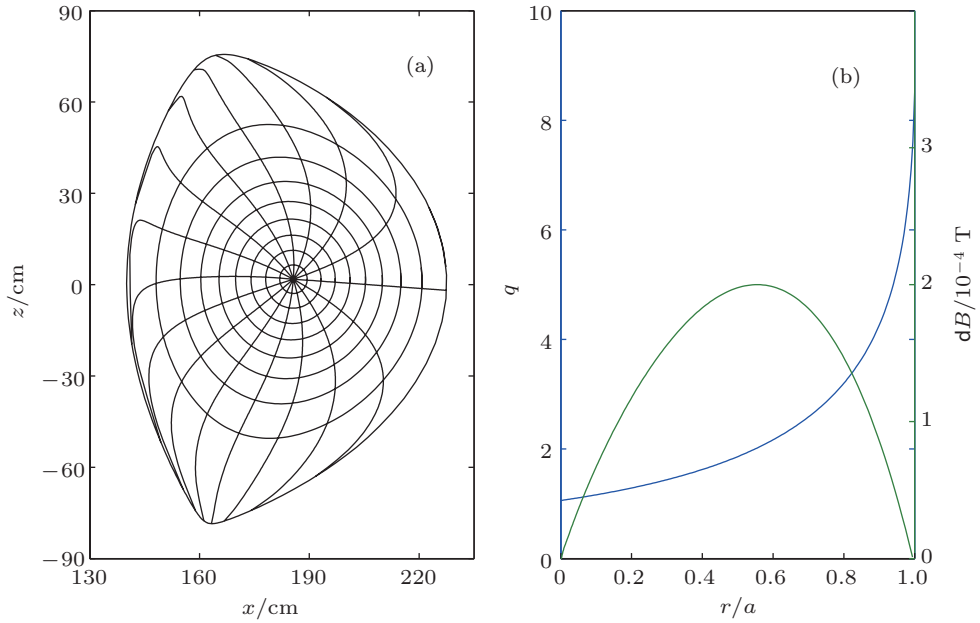


Fig. 1. (color online) (a) EAST equilibrium of shot 36662 in Boozer coordinate, (b) q profile and MHD perturbation profile used in corresponding modeling later.

2.1. First orbit loss

First orbit loss will always exist in tokamaks, including trapped loss, co- and counter-passing losses. Starting from the two constants of motion $E = \rho_{||}^2 B^2/2 + \mu B$ and $P_\varsigma = g\rho_{||} - \psi_p$, together with other conditions such as the trapped-passing boundary, and maximum and minimum magnetic field, we can obtain the orbit classification map.[15]

Figure 2(a) is the P_ς–μ plane of an 80-keV deuteron, in which each point represents a certain kind of orbit. The red line is the trapped-passing boundary. Points A, B, C stand for the most common three first loss orbits: counter-passing loss, trapped loss, co-passing loss. Their related orbits are shown in Fig. 2(b) with the same color. A peculiar first orbit loss type occurs in the overlap region of trapped loss and counter passing confined, a new domain where point D lies. The corresponding orbit is shown in Fig. 2(b) in red color. We considered this kind of orbit to be trapped loss. But instead of being lost immediately to the right wall, it first experiences a counter passing and then is lost to the left wall. This phenomenon happens in most EAST equilibriums, but is rarely seen in other tokamak equilibriums. To investigate them more explicitly, three-dimensional plots of the orbits in Fig. 2(b) are given in Fig. 3, in which the red orbit is the peculiar first orbit loss, while the blue and green ones are the familiar trapped loss and counter passing loss. First orbit loss often means particles lost before they finish a cycle in poloidal direction. Though it is common that passing particles run more than one cycle in the toroidal direction before being lost, it is quite novel that a newly trapped lost orbit would have the same character.

So in EAST tokamak the first orbit loss types include the classical counter-passing loss, trapped loss, and co-passing loss, in addition with the special trapped loss. As long as the domain of a certain orbit is located in the first orbit loss area in P_ς–μ plane, it will finally be lost.

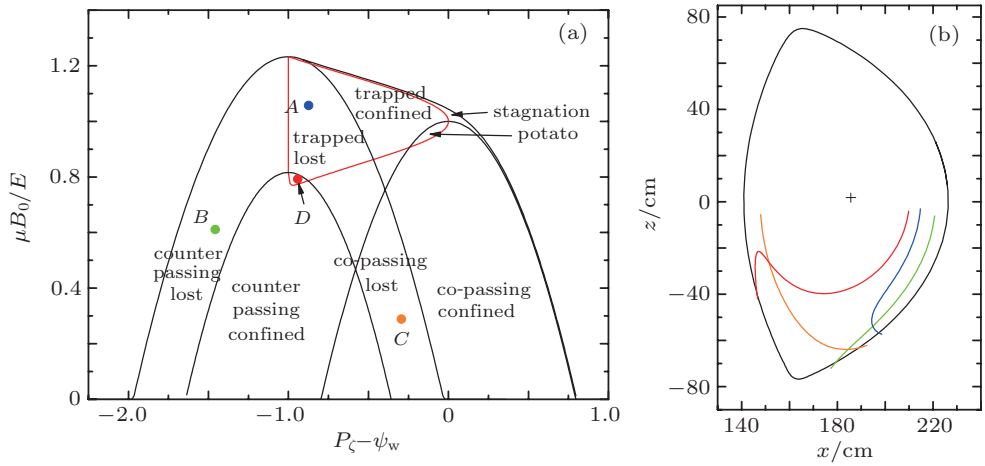


Fig. 2. (color online) (a) P_ζ–μ plane, showing the orbit types. (b) Four first orbit loss cases. A, B, C depict counter-passing loss, trapped loss, and co-passing loss, respectively. D is a particular case, which shows a first counter passing confined then trapped loss orbit. The orbits in Fig. 2(b) corresponding to the same colored dots in Fig. 2(a).

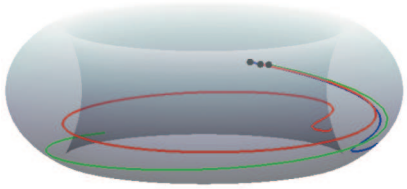


Fig. 3. (color online) Three-dimensional orbits corresponding to the same-colored ones in Fig. 2(b). The orbits in red, blue, green color represent peculiar trapped orbit loss, typical trapped loss, and counter-passing loss respectively.

2.2. MHD perturbations

The orbits of fast ions can be disturbed by MHD instabilities, and drifts can be relatively large especially when the orbits pass through the magnetic instability areas. The MHD perturbations can be represented by the form $\delta \boldsymbol{B} = \nabla \times \alpha(\psi, \theta, \zeta)\boldsymbol{B}$, which will lead to magnetic islands. Shown in Fig. 4 are the (2,1) and (3,2) magnetic islands in EAST, modeled with this form. The $\alpha(\psi, \theta, \zeta)$ profile implemented in the modeling has the form[16]

$$\alpha(\psi, \theta, \zeta) = \alpha_0 \left(\frac{x}{x_0}\right)^m \left(\frac{1-x}{1-x_0}\right)^{m(x_0^{-1}-1)} \sin(n\zeta - m\theta - \omega_n t), \quad (1)$$

where m and n are the typical poloidal and toroidal numbers, x_0 is the position of the magnetic island O point, and α_0 is often in 10^{-4} scale. A typical α profile for the (2,1) magnetic island is given in Fig. 1(b). Magnetic island width can be calculated with the expression[15]

$$\delta\psi = 4q\left(\frac{\alpha_{mn}}{s}\right)^{1/2}, \quad (2)$$

where $s = q'/q$ is the local shear, $q' = \mathrm{d}q/\mathrm{d}\psi_\mathrm{p}$.

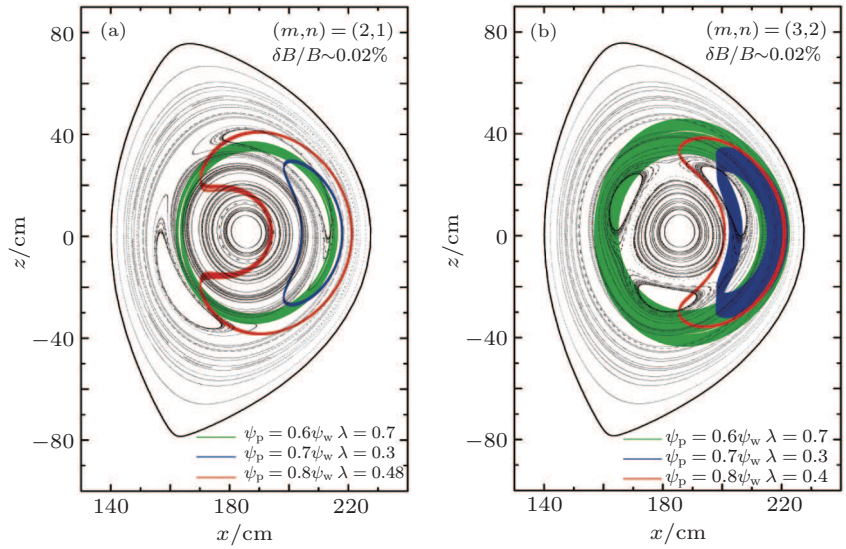


Fig. 4. (color online) The orbits under (a) (2,1) mode and (b) (3,2) mode; ψ_p is the initial flux surface position, while ψ_w is the last closed flux surface, and λ is the pitch angle.

Figure 4 depicts three representative orbits in the presence of (2,1) mode and (3,2) mode respectively. Big excursions can occur for both trapped and passing orbits, especially when they pass through the center of magnetic islands or spend enough time in the perturbed domain, as shown in Fig. 4(a) (red and green orbits) and Fig. 4(b) (blue and green orbits). For orbits which do not accept much perturbation the drift scales are much smaller, as can be seen from Fig. 4(a) (blue orbit) and Fig. 4(b) (red orbit). And for orbits which have no intersections with a magnetic island, little orbit excursion can be induced.

2.3. TF ripple

Toroidal field (TF) ripple is caused by the discreteness of the TF coils in tokamaks. Trapped particles in the presence of ripple can be lost through three processes: collisional ripple trapping, collisionless ripple trapping, and banana drift diffusion.[4] For thermal particles collisional ripple effects are important, while for energetic particles collisionless effects dominate.[17]

TF ripple magnitude in tokamaks can be defined by

$$\delta = (B_{\max} - B_{\min})/(B_{\max} + B_{\min}). \quad (3)$$

Shown in Fig. 5 is the ripple map for the EAST case, with δ in logarithmic scale.

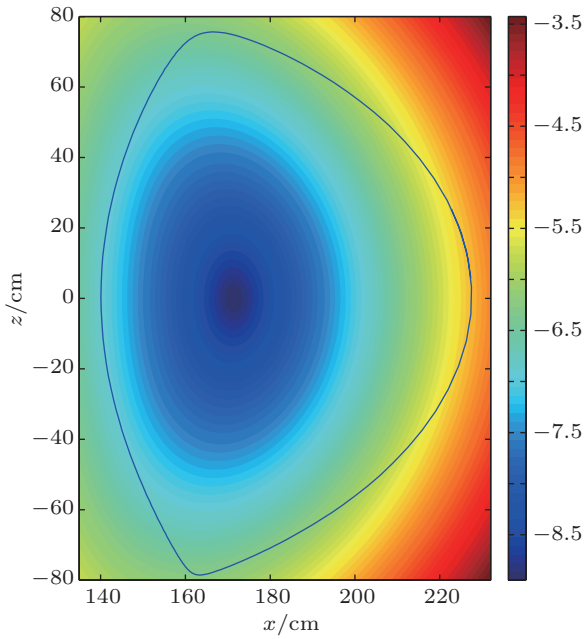


Fig. 5. (color online) EAST ripple map with δ in logarithmic scale.

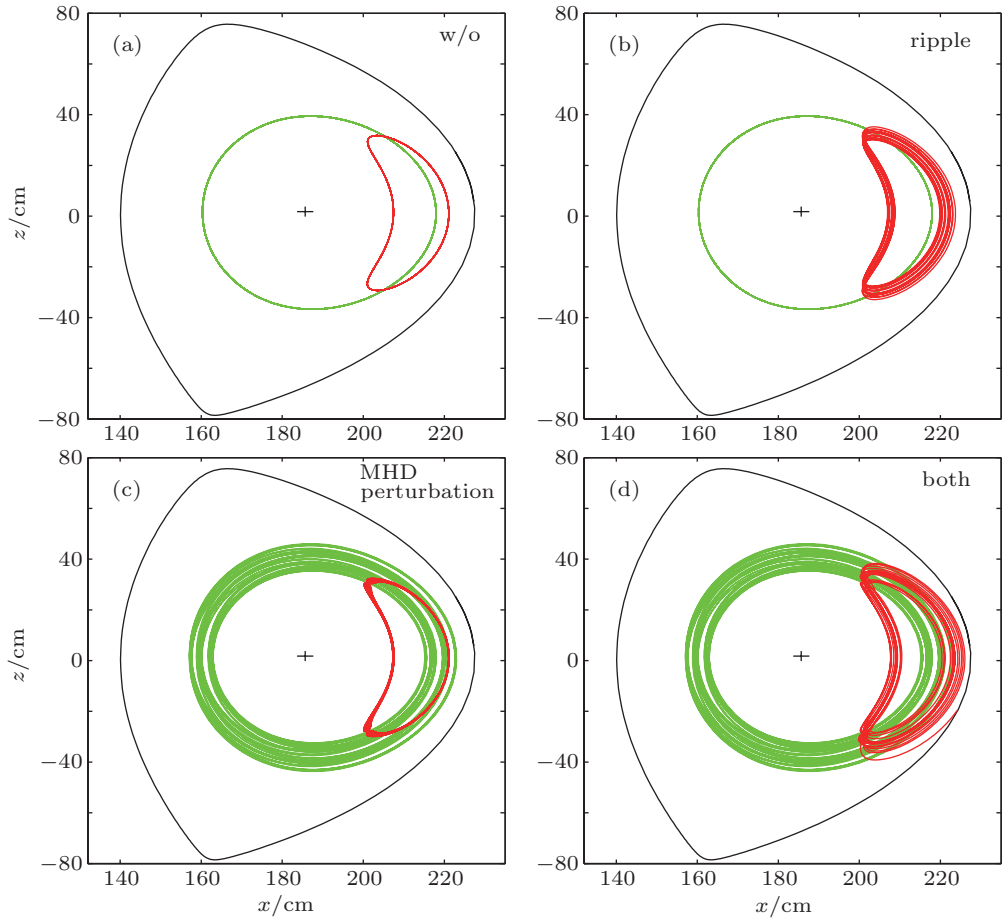


Fig. 6. (color online) Trapped (red) and passing (green) orbits with (a) no ripple, (b) in the presence of ripple, (c) with MHD perturbation, and (d) with both.

Figure 6 shows the disturbed trajectories when ripple, MHD perturbation, and both are added. The red trajectories are the trapped ones while the green orbits are the passing ones. Trapped orbits would be shifted outward in a significant scale under the influence of ripple, while the excursions caused by MHD perturbation are relatively small in this case. When both are added, the effect can be much more obvious, as can be seen from Figs. 6(b), 6(c), and 6(d). Furthermore, quantitative drift scales were calculated within 0.25 milliseconds, the results of which are shown in Fig. 7. The blue, green, and red curves depict the drift scale of orbits in Figs. 6(b), 6(c), and 6(d), respectively. It is readily apparent that the combined effect is much bigger than the effect of the ripple or MHD perturbation alone.

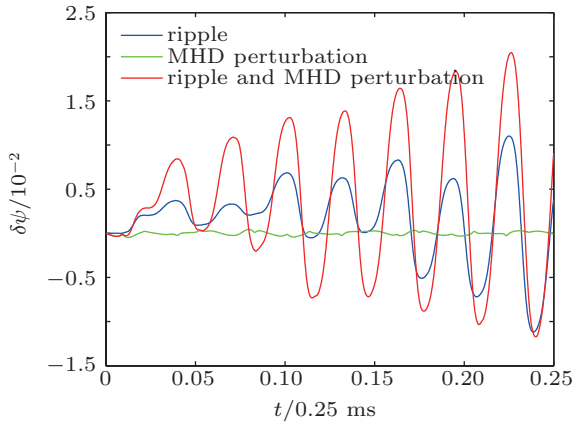


Fig. 7. (color online) The excursions of trapped orbits in Figs. 6(b) and 6(d).

3. Detailed studies and comparisons of drift orbits

3.1. Trapped passing boundary

Classical trapped-passing boundary condition has the form:[15]

$$E = \mu B(\psi_p, \theta), \quad P_\varsigma = -\psi_p, \quad 0 \le \theta \le \pi. \tag{4}$$

With further calculation we get

$$\frac{E}{B(\psi_p,\pi)} \le \mu \le \frac{E}{B(\psi_p,0)}, \tag{5}$$

$$\frac{E}{B(\psi_p,\pi)} \le \frac{E-\frac{1}{2}v_{||}^2}{B(\psi_p,\theta)} \le \frac{E}{B(\psi_p,0)}. \tag{6}$$

The right-hand side of Eq. (6) is always correct since $B(\psi_p,\theta)$ is always bigger than $B(\psi_p,0)$, so we only need to consider the left side. Thus a more experimental applicable trapped-passing boundary relationship can be worked out with the following form:

$$\lambda^2 \le \frac{B(\psi_p,\pi)-B(\psi_p,\theta)}{B(\psi_p,\pi)}. \tag{7}$$

The pitch angle λ in this paper is defined as $\lambda = v_{\|}/v$. The common pitch angle we talked about is actually $\arccos(\lambda)$. Orbits with their pitch angle satisfying the above equation are defined as trapped. For large aspect ratio tokamak $B(\psi_p,\pi) = B_0(1+\varepsilon)$ and $B(\psi_p,\theta) = B_0(1-\varepsilon)$; thus equation (7) becomes

$$\text{pitch}^2 \le \frac{2\varepsilon}{1+\varepsilon}, \tag{8}$$

where ε is the normal aspect ratio. This form is the same as the one derived by Brizar using another method.[18] Trapped orbits near the trapped-passing boundary can easily become passing under a little disturbance.

3.2. Orbit drifts versus pitch angle in different radial positions

The drift scale of orbits can be expressed as $\langle(\delta\psi_p)^2\rangle$. For particles with different pitch angles and radial positions, the orbit drifts are different. To have a deep understanding, we calculated the deviations of orbits in the presence of TF ripple and MHD perturbation in 0.075 millisecond (the transit time of the test particle is about 0.004 millisecond). Shown in Fig. 8 are the average orbit deviations versus pitch angle. Three different initial positions were chosen, which represent the inner, middle, and outer regions. Using Eq. (7) we can calculate the approximate pitch angle at the trapped-passing boundary, shown in Fig. 8 are the vertical dotted lines. Results imply that for particles near the center, the drift scales of orbits are much smaller than those near the boundary. For orbits in the inner part of plasmas ($\psi_p = 0.3\psi_w$), ripple will play a dominant role in disturbing trapped particles. For particles located in the middle region ($\psi_p = 0.55\psi_w$), both ripple and perturbation can be important. Ripple mainly affects on trapped particles,

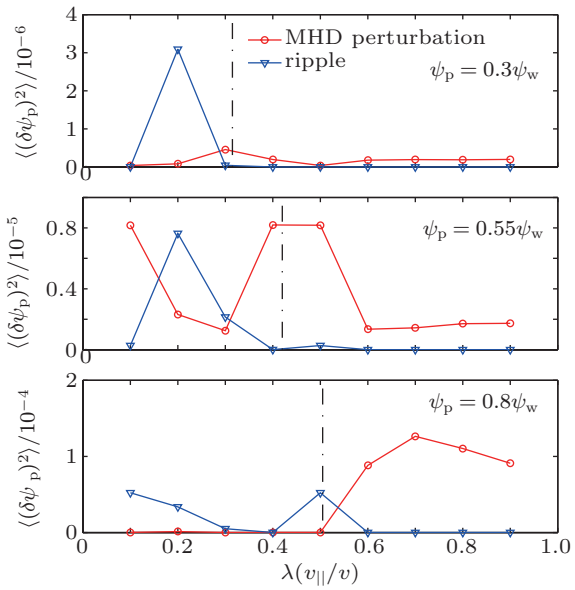


Fig. 8. (color online) Orbit deviations versus pitch angle at different radial positions. ψ_p is the initial flux surface and ψ_w is the last closed flux surface.

while MHD perturbation affects both trapped and passing particles. For particles in the outer region ($\psi_p = 0.8\psi_w$), we found ripple keeps playing an important role in the trapped ones, while MHD perturbation effects are only prominent for passing particles.

4. Domains of drift orbits in μ–P plane

Studies described in Subsection 3.2 give a comprehensive understanding of the orbit drift scale as a function of pitch angle in different positions, while for this section we simulated with multiple particle types to investigate the particle types influenced. The particles used here all have initial energies 80 keV and poloidal angles 0 or π, but have random pitch angles. Shown in Fig. 9 are the modeling results. The red points represent the particles that are ultimately lost, while the blue ones represent those confined. Note that all particles in the μ–P_ς plane represent their initial positions. Most lost particles in Fig. 9 belong to first orbit loss, since some initial particles are distributed near the boundary. Actually what we really care about are the red points in the confined domain, i.e., particles that are confined at the beginning but will be lost because of ripple or magnetic island effects. The results in Fig. 9 imply MHD perturbation can cause both co-passing and counter-passing particles loss, while TF ripple mainly causes some trapped particle loss.

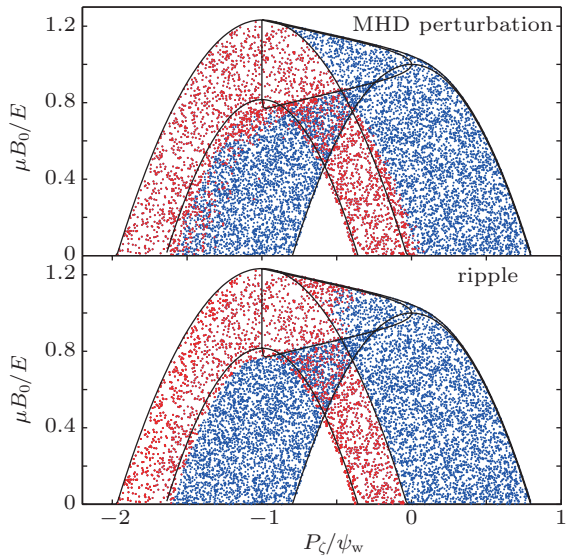


Fig. 9. (color online) Loss domain in μ–P_ς plane when one of the loss mechanisms is added. The red points are initial positions of particles which are ultimately lost, while the blue ones are those confined at last. The time used in modeling is 4.2 milliseconds.

Combining the modeling results in Subsections 3.2 and 3.3, we can conclude that the loss of trapped particles is mainly due to ripple, while the passing particles are mainly led to loss by magnetic perturbations.

5. Effects of important experimental parameters

Simulations were carried out to study important experimental factors. To make the work more representative and simple, we considered the fast particles induced by NBI. In EAST tokamak, we chose the NBI beam ions with injected beam power 4 MW and beam energy 80 keV as the source particles, which can be modeled by TRANSP code. Ten thousand particles were selected to represent the NBI source ions in the following simulations. To study the influences of experimental variables such as beta and q profile, we chose the experimental equilibriums from the same shot 36770 but at different moments in time. As indicated in Fig. 10, equilibriums at $t = 5.97$ and $t = 6.32$ have different β_p values but almost the same q profiles, and equilibriums at $t = 3.03$ and $t = 3.45$ have almost the same β_p values but different q profiles. The minor radius is almost the same in these four equilibriums. The time used in calculating the loss rates is 8 milliseconds, much shorter than the equilibrium transformational time.

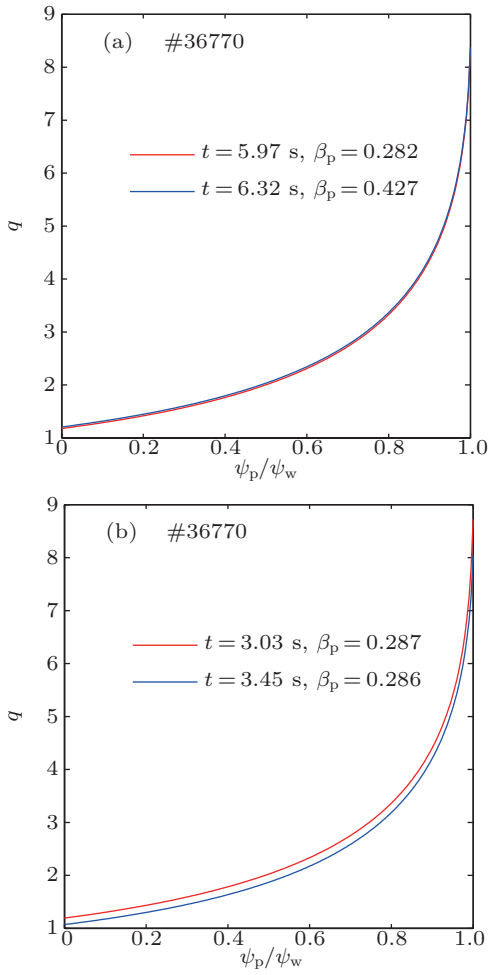


Fig. 10. (color online) The q profiles of different equilibriums, all from a same shot but different moments in time. Panel (a) shows almost same q profiles but different β_p values. Panel (b) shows almost same β_p values but different q profiles.

First, we studied the beta effect on particle confinement. As shown in Fig. 11, the solid lines are loss rates calculated using equilibrium with $\beta_p = 0.282$, while the dotted lines are calculated using equilibrium with $\beta_p = 0.427$. The red, blue lines represent loss rates when MHD perturbation and ripple effects are added respectively, the black lines refer to the loss rates when the two loss mechanisms are added simultaneously. As the results depict, in all cases, a larger β_p value can make the final loss smaller, which exactly meets the classical theory that a higher beta can improve the confinement.

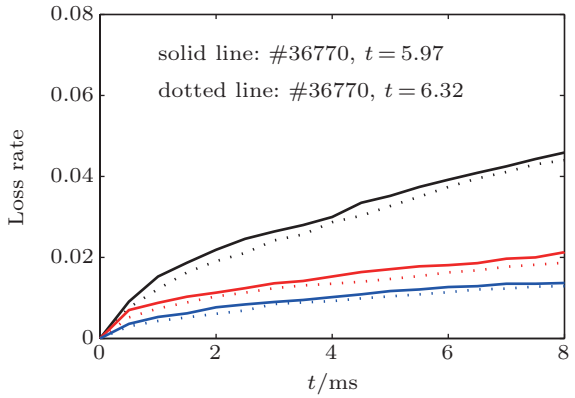


Fig. 11. (color online) The effect of β_p on particle confinement.

To investigate the properties of lost particles more explicitly, we plot them in the pitch angle and energy (λ–E) plane, as figure 12 shows. The red points represent the final positions of the lost particles, while the green ones represent the initial positions of the lost particles. Results demonstrate that lost particles with λ between -0.2 and 0.4 are mainly influenced by ripple, while those with λ ranging from 0.4 to 1 are mainly influenced by MHD perturbation. This also proves that ripple mainly affects the trapped particles, while MHD perturbation mainly affects the passing particles.

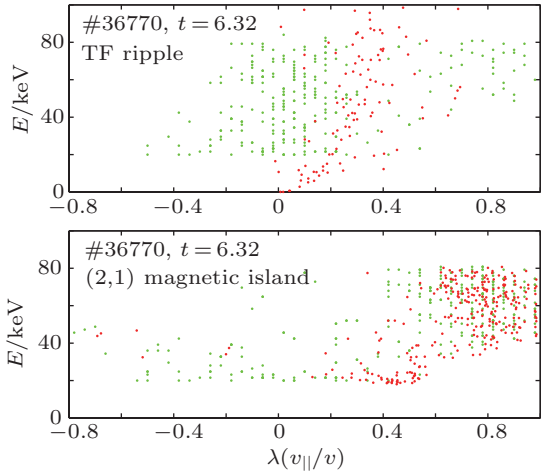


Fig. 12. (color online) Particle loss (green dots) caused by TF ripple and MHD perturbations, and their initial positions (red dots) in the pitch-energy plane.

To study the influence of q profiles on confinement, two equilibriums with different q profiles but the same beta value are used in the following modeling. Comparisons of the q profiles are shown in Fig. 10, with q_{95} equal to 5.566 in Fig. 10(a) and 5.311 in Fig. 10(b). Interestingly the losses induced by ripple are almost the same, but in case of MHD perturbations, the loss rates for equilibriums with a lower q_{95} become obviously higher, as depicted in Fig. 13.

To figure out the reason, we investigated the topologies of magnetic islands. The magnetic island widths are almost the same in the two cases, which are 3.06 cm at $t = 3.03$ s and 2.96 cm at $t = 3.45$ s. But further studies show the magnetic island topologies are different. As can be seen from Fig. 14, magnetic islands in panel (a) are more concentrated or localized than the ones in panel (b), and the lengths of magnetic islands in panel (b) are bigger than those in panel (a). This is especially important for passing particles that pass through the domain of magnetic islands, since these particles accept more disturbance if the magnetic islands are longer. Figure 15 shows the initial (red dots) and final (green dots) positions of the lost particles caused by magnetic perturbation in the pitch-energy plane. In Fig. 15(b) more particles with pitches between $0.5 \sim 1$ are lost, and these particles are mainly the passing ones. So we can conclude the magnetic islands in Fig. 14(b) cause more passing particles to be lost than those in Fig. 14(a). Besides, we took into account the initial particle numbers located in the magnetic islands. After calculations we found that more particles are inside and near the magnetic islands of Fig. 14(a) than those of Fig. 14(b). It seems that the magnetic islands in Fig. 14(a) have advantages in leading to bigger loss rates. But actually more losses are caused by magnetic islands in Fig. 14(b). So the topology of magnetic islands plays a dominant role in causing particle loss if the magnetic island widths are almost the same.

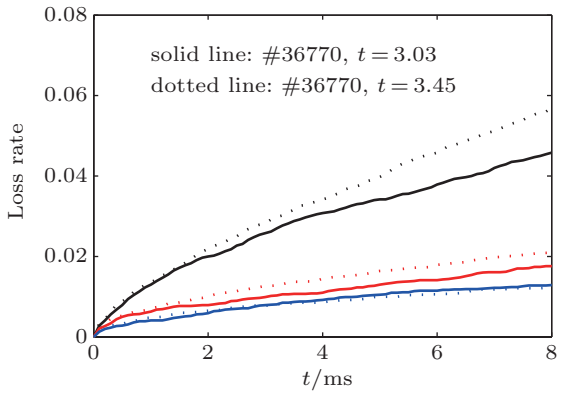


Fig. 13. (color online) The effect of q profile on particle confinement.

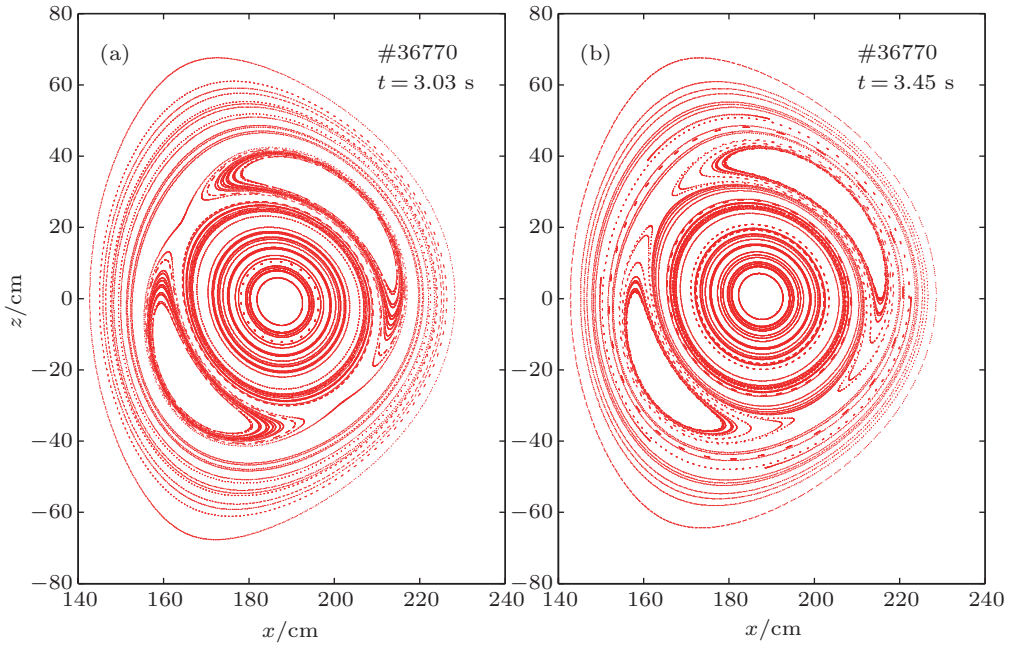


Fig. 14. (color online) Poincare plots of magnetic islands.

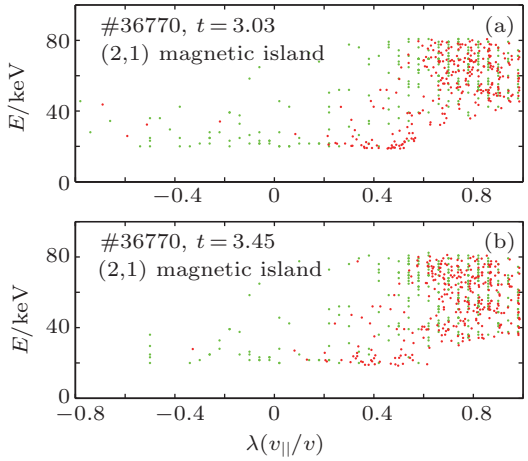


Fig. 15. (color online) Particles lost (green dots) due to MHD perturbation and their initial positions (red dots) in the pitch-energy plane.

6. Conclusion

In our studies we found that a specific first orbit loss exists apart from the classical types. This peculiar orbit first experiences a counter passing and then is lost like a trapped orbit. Drift orbits under the influence of ripple and magnetic islands are carefully studied. Each drift orbit caused by ripple or magnetic islands has its unique characteristics, based on which we can even identify a certain loss mechanism by analyzing the drift properties. The excursions of trapped orbits can be obviously larger when magnetic perturbations and ripple are added simultaneously. Orbit deviations are calculated in new ways as a function of pitch angle in different radial positions. From the modeling results we can conclude the loss of passing particles is mainly caused by MHD perturbations, while trapped particle loss is mainly due to the ripple. Big orbit drifts will occur when particles pass through the center of magnetic islands or spend enough time in the perturbed domain. In further simulations we calculated the loss rates, and proved that equilibriums with higher beta have a better capacity in particle confinement, while different q profiles can make the topologies of magnetic islands become different, and lead to different total losses.

References

[1] Jacquinot J, Putvinski S, Bosia G, *et al.* 1999 *Nucl. Fusion* **39** 2471

[2] Boozer A H 1980 *Phys. Fluids* **23** 2283

[3] Putvinskij S V, Tubbing B J D, Eriksson L G and Konovalov S V 1994 *Nucl. Fusion* **34** 495

[4] Goldston R J and Towner H H 1981 *J. Plasma Phys.* **26** 283

[5] White R B, Goldston R J, Redi M H and Budny R V 1996 *Phys. Plasmas* **3** 3043

[6] Redi M H, Budny R V, Darrow D S, Duong H H, Fisher R K, Janos A C, McChesney J M, McCune D C, Medley S S, Petrov M P, Schivell J F, Scott S D, White R B, Zarnstorff M C and Zweben S J 1995 *Nucl. Fusion* **35** 1509

[7] White R B, Zarnstorff M C and Zweben S J 1995 *Nucl. Fusion* **35** 1509

[8] Zweben S J, Darrow D S, Fredrickson E D, Taylor G, von Goeler S and White R B 1999 *Nucl. Fusion* **39** 1097

[9] Zweben S J, Darrow D S, Fredrickson E D, Taylor G, von Goeler S and White R B 1999 *Nucl. Fusion* **39** 1097

[10] Udintsev V S, van Milligen B P, Schuller F C, Kramer-Flecken A, Donne A J H, van Gorkom J C, Domier C W and team T 2003 *Nucl. Fusion* **43** 1424

[11] García-Muñoz M, Fahrbach H U, Günter S, Igochine V, Mantsinen M, Maraschek M, Martin P, Piovesan P, Sassenberg K and Zohm H 2008 *Phys. Rev. Lett.* **100** 055005

[12] Gobbin M, Marrelli L, Fahrbach H U, Garcia-Munoz M, Guenter S, Martin P, White R B and Team A U 2009 *Nucl. Fusion* **49** 095021

[13] White R B and Chance M S 1984 *Phys. Fluids* **27** 2455

[14] White R B 1990 *Phys. Fluids B: Plasma Phys.* **2** 845

[15] White R B 2001 *The Theory of Toroidally Confined Plasmas*, 3nd edn. (London: Imperial College Press) pp. 63–81

[16] Mynick H E 1993 *Phys. Fluids B: Plasma Phys.* **5** 1471

[17] Wesson J 2004 *Tokamaks*, 3nd edn. (New York: Oxford University Press) p. 176

[18] Brizard A J 2011 *Phys. Plasmas* **18** 022508